J. CHEM. SOC. FARADAY TRANS., 1994, 90(18), 2627–2634

Photoinduced and Thermal Isomerization Processes for Bis-Oxonols: Rotor Volume, Stereochemical and Viscosity Effects

Andrew C. Benniston and Anthony Harriman*
Center for Fast Kinetics Research, The University of Texas at Austin, Austin, TX 78712, USA

Four bis-oxonols have been synthesized which possess different alkyl substituents appended to the thiobarbiturate subunit. The nature of the alkyl substituent affects the photophysical properties of the dye in solution since it modulates the rate of rotation of the thiobarbiturate subunit around one of the double bonds in the connecting trimethine bridge. Rates of light-induced (*trans* to *cis*) and thermal (*cis* to *trans*) isomerization processes have been measured for one of the dyes in protic (*i.e.* alkanols) and aprotic solvents at various temperatures. These rates, together with activation energies derived from Arrhenius plots, are discussed in terms of the hydrogen bonding and stereochemical properties of the solvent. The thermal step is very sensitive to the stereochemistry of the solvent while the light-induced process is controlled mostly by the size of the rotor and the solvent viscosity. The overall effects may be explained, at least in a qualitative sense, in terms of the medium-enhanced barrier model.

Relative changes in fluorescence intensity are commonly used in biophysics to probe local environments and to monitor concentrations of intracellular species. Fluorescent dyes that undergo facile photoisomerization are of particular interest as molecular probes because the fluorescence properties can be extremely sensitive to the environment.[1] Indeed, such dyes are often employed to elicit information regarding membrane fluidity, viscosity, polarity, potential and phase-transition temperature[2] while related dyes have been used to determine intracellular pH and specific ion concentrations[3] and to stain microbes, antibodies, proteins *etc.*[4] The design of new biophysical probes is aided considerably if the mechanism of the isomerization process is well understood and if the nature of any interaction between dye and adjacent solvent molecules can be identified. However, the mechanisms for light-induced isomerization reactions can be surprisingly complex,[5] especially for polar molecules,[6] and there is still considerable debate over how best to describe friction between the twisting groups and adjacent solvent molecules.[7] The photoisomerization of stilbene, for example, has been studied continuously for the past 30 years and is still under debate.[8]

Here, we consider the dynamics of light-induced and thermal isomerization reactions for some bis-oxonols in polar organic solvents. Such compounds have long been used in the colourimetric analysis of lipoperoxides formed by *in situ* oxidation of lipid membranes[9] and for the fluorimetric determination of membrane potentials.[10] Indeed, it has been reported that there is a 20-fold increase in fluorescence yield upon binding to membranes or proteins, without an apparent change in absorption or fluorescence maxima.[11] More recent studies[12] have shown that bis-oxonols undergo photoisomerization from the first excited singlet state on the timescale of a few hundred picoseconds. The resultant isomer reverts to the initial configuration over some tens of microseconds. We have now examined these isomerization steps in more detail using a small series of bis-oxonols, more correctly named as 5,5′-(prop-1-en-1-ylidiene(bis(*N*,*N*′-dialkyl-2-thiobarbituric acid) derivatives. The objective of this work was to identify the major parameters that influence the rates of isomerization in these (supposedly) simple compounds in polar solvents.

Experimental

Starting materials were purchased from Aldrich or Eastman-Kodak and were used as received. Synthesis of compounds

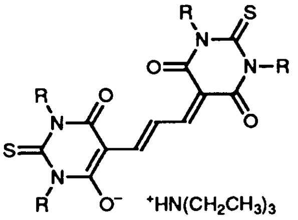

1: R = C_2H_5
2: R = C_3H_7
3: R = C_4H_9
4: R = C_6H_{13}

1[13] and **3**[12] (in its protonated form, not as a triethylammonium salt) has been described previously while compounds **2** and **4** were prepared by simple modification of the method used to prepare **3**. Reaction involved the triethylamine-catalysed condensation of a thiobarbituric acid with the corresponding 5-(3-methoxyprop-1-en-2-ylene)barbituric acid and was followed by absorption spectroscopy.[12] Each dye was purified by extensive chromatography on silica using ethyl acetate as eluent and was analysed by ^1H NMR, TLC and FAB mass spectrometry. Compound **3** was further analysed by exact mass spectrometry, elemental analysis, ^{13}C NMR and FTIR. Intermediate reagents were routinely analysed by TLC and ^1H NMR. Preparation of reagents needed for synthesis of the hexyl derivative **4**, the most exotic of the new compounds, is described below while the corresponding reagents for synthesis of **2** were prepared by the same route starting with propylamine.

Preparation of Hexyl Isothiocyanate

Hexylamine (20 g, 200 mmol) was added dropwise to a stirred solution of CS_2 (15 g, 200 mmol) and NaOH (8 g, 200 mmol) in water (50 ml) maintained at 10–15 °C. The mixture was subsequently heated to 100 °C for 2 h. After the mixture had been cooled to 35–40 °C, ethyl chlorocarbonate (21.6 g, 200 mmol) was added and the mixture was stirred for 30 min. The organic layer was separated, dried over Na_2SO_4 and distilled to give a colourless liquid. Yield: 21 g (75%). ^1H NMR ($CDCl_3$): δ 0.85–0.89 (t, 3 H, *J* 6.7 Hz); 1.25–1.44 (m, 6 H); 1.61–1.69 (m, 2 H); 3.46–3.51 (t, 2 H, *J* 6.6 Hz).

Preparation of *N*,*N*′-Dihexylthiourea

Hexylisothiocyanate (10 g, 70 mmol) was added over a period of 1 h to a stirred solution of hexylamine (10.5 g, 104 mmol) in water (50 ml). The mixture was stirred overnight and the organic layer was extracted with CH_2Cl_2 (100 ml). After it had been dried with $MgSO_4$, the organic layer was evaporated under vacuum and the residual oil was freeze-dried overnight. The solid residue was recrystallized from hexane as a while solid. Yield: 10 g (59%). ^{1}H NMR ($CDCl_3$): $\delta = 0.86$–0.89 (t, 6 H, *J* 6.7 Hz); 1.30–1.57 (m, 12 H); 1.60 (m, 4 H); 3.39 (t, 4 H, *J* 6.5 Hz); 5.7 (broad, 2 H, N—H).

Preparation of *N*,*N*′-Dihexyl-2-thiobarbituric Acid

N,*N*′-Dihexylthiourea (5 g, 20.5 mmol) was added to a freshly prepared solution of sodium ethoxide [1 g Na in absolute ethanol (50 ml)] and diethylmalonate (6.6 g, 41 mmol). The mixture was heated under reflux with strong agitation and a constant flow of N_2 for 3 days. After the mixture had been cooled to room temperature, water (50 ml) was added slowly before the ethanol was removed by distillation. The residue was poured into water (100 ml), cooled, and filtered. The filtrate was acidified with dilute hydrochloric acid and the aqueous solution was subsequently extracted with CH_2Cl_2 (3 × 100 ml). The combined organic layers were dried with $MgSO_4$ and evaporated to dryness. The resultant red oil was purified by gravitational chromatography on silica gel with CH_2Cl_2–hexane 1 : 1 as eluent to give a yellow oil which solidified upon standing. Yield: 2.6 g (41%). ^{1}H NMR ($CDCl_3$): δ 0.85–0.90 (t, 6 H, *J* 6.7 Hz); 1.29–1.44 (m, 12 H); 1.56–1.66 (m, 4 H); 3.69 (s, 2 H); 4.27–4.33 (t, 4 H, *J* 7.7 Hz).

Preparation of *N*,*N*′-Dihexyl-2-thio-5-(3-methoxyprop-1-en-2-ylene)barbituric Acid

To a vigorously stirred solution of 1,3,3-trimethoxyprop-1-ene (5.5 g, 42 mmol) in methanol (20 ml) was added rapidly *N*,*N*′-dihexylthiobarbituric acid (2.6 g, 8.3 mmol). The precipitate was quickly removed by filtration and dried under vacuum. Yield: 2.2 g (69%). ^{1}H NMR ($CDCl_3$): δ 0.79–0.85 (t, 6 H, *J* 6.5 Hz); 1.27 (m, 12 H); 1.62 (m, 4 H); 3.89 (s, 3 H); 4.31–4.38 (q, 4 H, *J* 7.6 Hz); 7.38–7.52 (q, 2 H, *J* 12.7 Hz); 8.02–8.06 (d, 1 H, *J* 11.6 Hz).

^{1}H NMR spectra were recorded with a Bruker WH250 FT-NMR instrument with TMS as internal standard. Absorption spectra were recorded with a Hitachi U3210 spectrophotometer and fluorescence spectra were recorded with a fully corrected Perkin-Elmer LS5 spectrofluorimeter. Solutions for fluorescence studies were adjusted to possess an absorbance of <0.05 at the excitation wavelength of 510 nm. All temperature dependence studies were made with the sample cuvette housed in a thermostatted metal block having a thermocouple maintained in direct contact with the solution. Singlet excited-state lifetimes were measured with a synchronous streak-camera following excitation at 532 nm with a 30 ps laser pulse. Approximately 100 individual traces were averaged and analysed by non-linear, least-squares computer iteration, after deconvolution of the instrumental response function. The time resolution of this instrument was *ca.* 40 ps. Solutions were adjusted to possess an absorption of *ca.* 0.15 at 532 nm and were deoxygenated by purging with N_2. Fluorescence was isolated from scattered laser light with a 532 nm notch filter used in conjunction with narrow band-pass filters selected to isolate a 10 nm wide spectral window at 600 nm.

Flash photolysis studies were made with a frequency-doubled Quantel YG481 Nd : YAG laser (pulse width 10 ns; pulse energy 40 mJ). Solutions were adjusted to possess an absorbance of *ca.* 0.2 at 532 nm and were purged with N_2, O_2 or air according to the needs of the experiment. Transient differential absorption spectra were recorded point-by-point with five individual laser shots being averaged at each wavelength. Kinetic studies were made at fixed wavelength with 50 individual laser shots being averaged and analysed by computer non-linear, least-squares iterative procedures. Where necessary, the laser intensity was attenuated with crossed-polarizers. Transient differential absorption coefficients were measured by the complete bleaching method and the laser intensity was calibrated using zinc *meso*-tetraphenylporphyrin in benzene as standard.[14,15]

Results

Structure of the Ground State

The authenticity of **3** was established by ^{1}H and ^{13}C NMR in $CDCl_3$, exact mass spectrometry and elemental analysis. Furthermore, the presence of the *N*,*N*,*N*-triethylammonium cation was clearly apparent in the ^{1}H NMR spectrum. From examination of space-filling molecular models,[13] it was concluded that a *trans* arrangement of the protons in the trimethine bridge was much preferred over the *cis* isomer due to the reduced degree of steric crowding. This finding was fully supported by high-resolution ^{1}H NMR spectroscopy carried out in $CDCl_3$ solution. Close inspection of the coupling constants observed for the trimethine protons, which are easily identified from their particular chemical shifts,[16] allows complete assignment of the ground-state structure. Thus, the ^{1}H NMR spectrum shows a doublet (corresponding to two protons) and a triplet (corresponding to one proton) at 8.14 and 8.54 ppm, respectively, with identical coupling constants of 13.8 Hz (Fig. 1). Such a pattern is consistent with either an all-*cis* or an all-*trans* orientation of the trimethine protons. Since an all-*cis* protonic configuration cannot be accommodated, the ground state must adopt an all-*trans* proton arrangement. The other bis-oxonols showed identical ^{1}H NMR spectral patterns for the trimethine bridge and, therefore, they are also believed to possess the *trans* geometry in the ground state.

Furthermore, the two terminal methine protons are equivalent, suggesting complete delocalization of the negative charge over all four oxygen atoms. This finding appears consistent with FTIR spectra recorded in $CHCl_3$ since only a single C=O stretching band was observed (at 1635 cm^{-1}), together with C=C (at 1604 cm^{-1}) and C=S (at 1510 cm^{-1}) stretching vibrational bands. The C—N amide bonds should also be considered as possessing partial double-bond character, hence bringing the terminal C=S bond into partial conjugation with the trimethine bridge. There is, therefore,

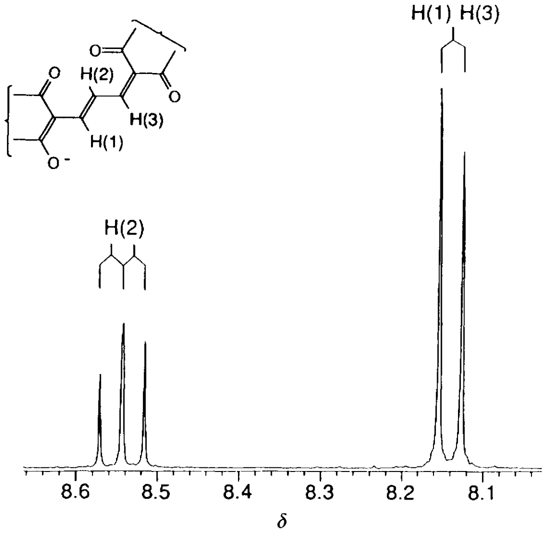

Fig. 1 ^{1}H NMR spectrum recorded for bis-oxonol **3** in $CDCl_3$ showing the trimethine protons and their assignment

extended π-electron conjugation throughout the entire molecule and numerous resonance forms can be drawn; two such forms are shown below. Finally, the bond order of the C atoms in the trimethine bridge must be *ca.* 1.5.

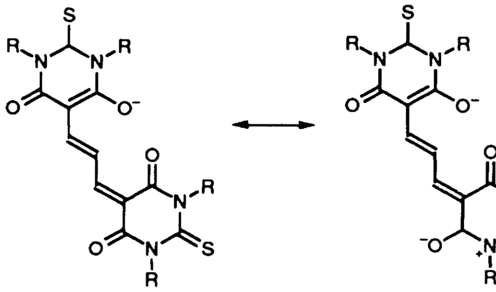

Further examination of space-filling molecular models indicates that twisting of the central trimethine bridge, to form the corresponding *cis* isomer, involves considerable steric strain. Indeed, there is marked steric crowding between H(2) and the O atoms on the rotor. The resultant *cis* isomer appears to be slightly non-planar, suggesting that conjugation between the terminal oxonol groups will be less pronounced than in the *trans* isomer. The *N*-alkyl groups are not responsible for this steric crowding and, therefore, the activation barrier for isomerization might be expected to be only weakly dependent on the size of these substituents. One of many likely resonance forms for the *cis* isomer is shown below:

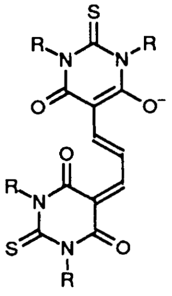

Photophysical Properties in Ethanol

Absorption and fluorescence spectral profiles recorded for **3** in dilute ethanol solution are shown in Fig. 2. The fluorescence excitation spectrum gave a good match to the absorption spectrum while the Stokes' shift, measured in dilute ethanol solution, was 620 ± 30 cm^{-1} which indicates the absence of substantial geometric changes upon promotion to the first excited singlet state. The fluorescence quantum yield (Φ_f), measured relative to Rhodamine 101 in ethanol,[17] was found to be 0.084 ± 0.008 and the radiative lifetime, calculated from the Strickler–Berg expression,[18] was derived as 2.15 ± 0.15 ns. The fluorescence lifetime (τ_s) was found to be 180 ± 10 ps by laser-induced fluorescence spectroscopy.

Laser flash photolysis studies carried out in N_2-saturated ethanol solution have been described previously[12] and indicate that the triplet state is formed in extremely low quantum yield (*i.e.* <0.001). A second transient, which absorbs strongly at 565 nm (Fig. 3) and which does not react with oxygen, is believed to be a geometric isomer formed by rotation around one of the central double bonds.[12] No other transient species were observed in the decay records and, following excitation with a 30 ps laser pulse at 532 nm, it was confirmed that the isomer was produced directly from the first excited singlet state. By completely bleaching the dye with a saturating laser pulse at 532 nm in the presence of oxygen, the differential molar absorption coefficient for the isomer at its differential absorption maximum of 565 nm was found to be $(1.5 \pm 0.2) \times 10^4$ l mol^{-1} cm^{-1}. Using this value, the quantum yield for formation of the *cis* isomer (Φ_i) was derived to be 0.65 ± 0.07. By correcting the differential transient absorption spectrum (Fig. 3) for depletion of the ground state (Fig. 2), the corrected absorption spectrum for the *cis* isomer was compiled and is compared with that of the *trans* form in Fig. 4. It is clear that the *cis* isomer absorbs somewhat to the red of the ground state with a significantly lower maximum absorption coefficient. Such spectral changes are consistent with decreased overlap of the π-electronic orbitals[19] caused by the deviation from planarity that accompanies conversion from *trans* to *cis* isomers. This effect is associated with stereochemical inhibition of resonance.

Photophysical measurements made with the other dyes in ethanol solution showed very similar behaviour. The nature of the substituent did not affect the absorption or fluorescence spectral profiles nor the molar absorption coefficient measured at the absorption peak of 540 nm. The derived lifetimes and quantum yields are collected in Table 1 and it is seen that the nature of the alkyl substituent appended to the thiobarbiturate subunit exerts only a modest effect on the photophysical properties. In particular, increasing the length of the alkyl substituent causes a progressive increase in both Φ_f and τ_s, without affecting the magnitude of the Stokes' shift. There was a corresponding increase in the yield of the unstable isomer with increasing length of the alkyl substitu-

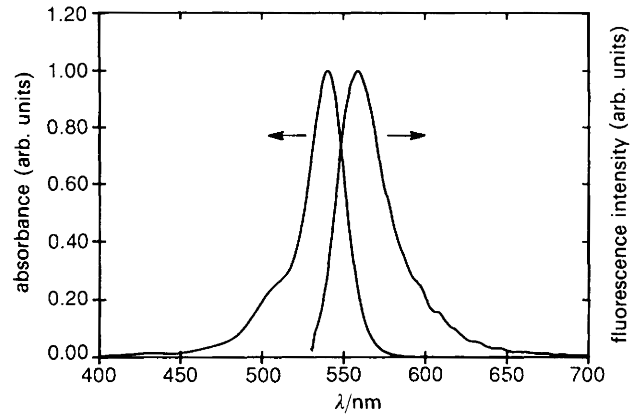

Fig. 2 Absorption and fluorescence spectra recorded for bis-oxonol **3**, in dilute ethanol solution. The excitation wavelength used for the fluorescence spectrum was 510 nm.

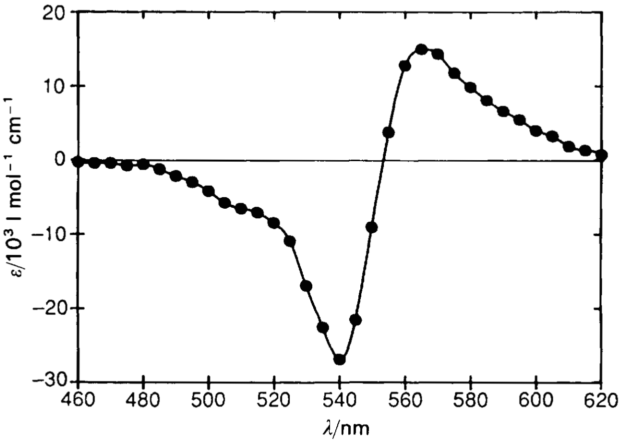

Fig. 3 Differential absorption spectrum recorded 1 μs after excitation of bis-oxonol **3** in O_2-saturated ethanol solution with a 10 ns laser pulse at 532 nm. The transient species is believed to be the *cis* isomer.

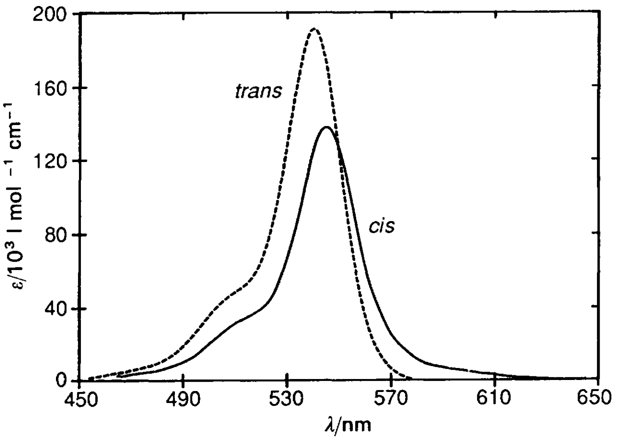

Fig. 4 Comparison of absorption spectra for the *trans* (– – –) and *cis* (——) isomers of bis-oxonol **3** in ethanol solution

ent and a modest variation in its lifetime. In each case, the triplet quantum yield was <0.001. Similar behaviour was observed in acetonitrile solution.

Photophysical Properties of 3 in Different Solvents

The principal route for deactivation of the first excited singlet state of the bis-oxonols involves isomerization of one of the bonds in the trimethine bridge. This process is expected to require large-scale torsional motion and to involve frictional forces with adjacent solvent molecules. In order to assess the magnitude of such interactions, the photophysical properties of **3** were recorded in a series of solvents of differing viscosity and/or polarity. Radiative lifetimes (τ_f) were calculated from the Strickler–Berg expression[18] for each solvent ($1/\tau_f = 2.5n^2 \times 10^8$ s^{-1}, where n is the solvent refractive index at 550 nm). It was observed that the absorption and fluorescence spectral profiles and peak maxima were only slightly affected by changes in solvent and that the Stokes' shift remained essentially independent of solvent polarity (Table 2). These findings can be used to infer that there is no significant change in dipole moment upon excitation to the first excited singlet state.[6] Both the fluorescence quantum yield and excited singlet state lifetime were found to depend on the nature of the solvent (Table 2), indicating a solvent effect on the rate of non-radiative deactivation of the singlet state. The triplet quantum yield remained <0.005 in all solvents studied while the quantum yield for formation of the *cis* isomer (Φ_i) was dependent on the identity of the solvent (Table 2). The results indicate clearly that formation of the *cis* isomer and fluorescence are in competition. The lifetime of the *cis* isomer was also found to be solvent dependent (Table 2).

Discussion

Effect of Changing the Volume of the Rotor

The molar volumes of the rotating groups (V_m) for the various bis-oxonols were calculated[20] and the derived values are col-

Table 1 Photophysical properties measured for the various bis-oxonols in dilute ethanol solution

compound	$\lambda_{max}{}^a$/nm	log($\varepsilon_{max}{}^b$/l mol^{-1} cm^{-1})	$\Phi_f{}^c$	$\tau_s{}^d$/ps	$\Phi_i{}^c$	$\tau_i{}^e$/μs	$V_m{}^f$/ml mol^{-1}
1	538	5.28	0.058	125	0.68	9.6	100
2	540	5.27	0.066	140	0.66	10.6	120
3	540	5.28	0.084	180	0.65	11.8	140
4	540	5.22	0.100	210	0.62	13.3	180

[a] Absorption maximum, ±1 nm. [b] Molar absorption coefficient at the absorption maximum, ±6%. [c] ±10%. [d] ±10 ps. [e] ±0.2 μs. [f] Molar volume.

Table 2 Photophysical properties of bis-oxonol **3** in various solvents at 22 °C

solvent	η/cP	$\lambda_{max}{}^a$/nm	SS^b/cm^{-1}	$\Phi_f{}^c$	$\tau_s{}^d$/ps	$\Phi_i{}^e$	$\tau_i{}^f$/μs
methanol	0.632	538	700	0.055	125	0.71	9.8
ethanol	1.132	540	665	0.084	180	0.65	11.8
propan-1-ol	1.970	540	690	0.112	240	0.63	13.3
butan-1-ol	2.607	541	620	0.131	250	0.63	14.5
pentan-1-ol	3.441	541	620	0.140	300	0.60	15.4
hexan-1-ol	4.547	542	650	0.157	340	0.58	16.7
decan-1-ol	11.542	543	660	0.200	430	0.55	20.8
propan-2-ol	3.421	540	670	0.135	290	0.61	19.4
butan-2-ol	3.042	541	680	0.125	270	0.62	22.3
isobutyl alcohol[g]	3.446	542	690	0.130	295	0.61	12.2
tert-butyl alcohol[h]	4.420	541	665	0.180	380	0.57	33.2
pentan-2-ol	3.390	542	655	0.138	300	0.60	22.6
pentan-3-ol	4.024	542	670	0.170	365	0.57	26.5
isopentyl alcohol[i]	3.786	543	665	0.135	290	0.61	12.7
2-methylbutan-1-ol	4.460	541	670	0.150	320	0.61	13.7
cyclohexanol	56.5	543	680	0.375	800	0.17	22.9
glycerol	141.2	544	700	0.495	1040	0.02	—
acetonitrile	0.345	540	700	0.090	195	0.66	47.8
DMSO	1.996	545	650	0.180	380	0.52	57.8
acetone	0.304	539	635	0.105	230	0.61	36.4
diethyl ether	0.242	542	655	0.080	195	0.70	35.2
ethyl acetate	0.455	541	630	0.130	275	0.61	36.5
propylene carbonate	2.53	540	670	0.200	420	0.51	49.0
1,4-dioxane	1.439	540	650	0.160	345	0.54	46.3
nitromethane	0.608	542	660	0.125	270	0.62	38.5
DMF	0.924	540	670	0.150	315	0.65	45.2

[a] Absorption maximum, ±2 nm. [b] Stokes' shift, ±25 cm^{-1}. [c] ±7%. [d] ±10 ps. [e] ±10%. [f] ±0.2 μs. [g] 2-Methylpropan-1-ol. [h] 2-Methylpropan-2-ol. [i] 3-Methylbutan-1-ol.

lected in Table 1. Replacing the ethyl substituents with hexyl groups almost doubles the molar volume of the rotor and is accompanied by modest decreases in the rates of isomerization. In fact, the rates of both light-induced ($k_s = 1/\tau_s - 1/\tau_f$) and thermal ($k_t = 1/\tau_i$) isomerization processes correlate reasonably well with the inverse of the molar volume throughout this small series of bis-oxonols (Fig. 5) according to

$$\log k_{\mathrm{isom}} \approx A/V_{\mathrm{m}} \qquad (1)$$

where k_{isom} relates to k_s or k_t and A is the rate of isomerization for a (hypothetical) infinitely large rotor. This finding is consistent with isomerization involving large-scale torsional motion and suggests that the rate of isomerization should depend on frictional forces with surrounding solvent molecules.[7] From the intercepts to Fig. 5, rates of isomerization with infinitely bulky substituents are extrapolated to be *ca.* 2×10^9 and *ca.* 5×10^4 s^{-1}, respectively, for light-induced and thermal isomerizations in ethanol at 22 °C. The slopes to Fig. 5 are quite disparate, that for light-induced isomerization (*i.e.* 57 mol ml^{-1}) being almost double that for the thermal process (*i.e.* 32 mol ml^{-1}). Such behaviour indicates that photoisomerization is more sensitive towards frictional forces with adjacent solvent molecules than is the corresponding dark reaction. Comparable behaviour was observed in ethanol and acetonitrile solutions, although the slopes of plots to eqn. (1) were significantly smaller (*i.e.* 40 and 17 mol ml^{-1}. respectively, for light-induced and thermal steps) in the aprotic solvent. This latter effect may arise from closer packing of a hydrogen-bonding solvent around the bis-oxonol molecule.

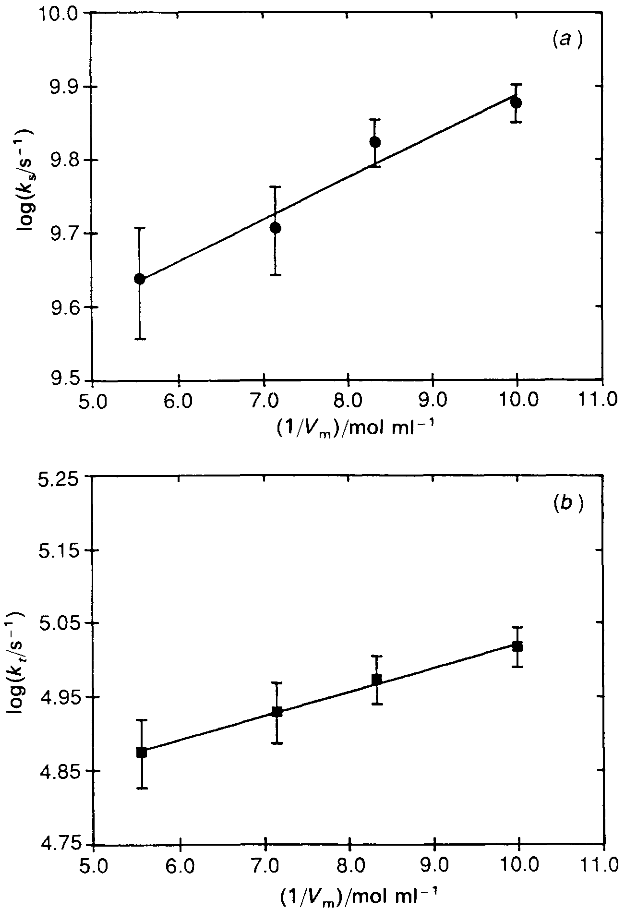

Fig. 5 Correlation between rate of isomerization and the inverse of the molar volume of the rotor for (*a*) light-induced and (*b*) thermal isomerization processes for the various bis-oxonols in ethanol

Photoisomerization in Alkanol Solvents

The dynamics for isomerization of polar molecules may depend on viscosity[21] and/or polarity[22] of the solvent. Many studies have shown that shear viscosity (η) often provides a poor description of the extent of friction between a rotor and adjacent solvent molecules and the concept of microviscosity has been introduced as an alternative.[23] Similarly, solvent polarity can be presented by the $E_T(30)$ parameter,[24] although this may not be entirely satisfactory in all cases. Within these limitations, the rate of isomerization (k_{isom}) can be expressed in terms of the following general equation:

$$k_{\mathrm{isom}} = (B/\eta^{\alpha})\exp(-E_A/RT)\exp\{\beta[E_T(30) - 30]\} \qquad (2)$$

The β term describes the dependence of the barrier height E_A on solvent polarity,[22] whereas the latter parameter corresponds to the inherent (polarity-independent) activation energy. The α term allows for a power dependence in the effect of viscosity on the rate of isomerization[21] while the pre-exponential factor B corresponds to the activationless rate of isomerization in a non-polar solvent having unit viscosity. Steady-state absorption and fluorescence spectra recorded for the bis-oxonols appear independent of solvent polarity (Table 2) suggesting that, at least to a first approximation, $\beta \approx 0$. We consider, therefore, that the dynamics of light-induced and thermal isomerization steps are essentially independent of solvent polarity.

Fitting the derived rates of light-induced isomerization (k_s) as obtained at 22 °C in alkanols of differing viscosity[25] to eqn. (2) with $\beta = 0$ gave a linear plot over a very wide viscosity range (Fig. 6). Therefore, within the quality and quantity of the available kinetic data, shear viscosity gives an appropriate measure of microfriction for this system. For the light-induced isomerization process, the power coefficient α has a value of 0.51 ± 0.01. The intercept to this plot corresponds to $\ln(B - E_A/RT)$ and has a value of 22.45. It is interesting to note that kinetic data collected in most of the alcohols, including cyclohexanol, glycerol and several branched alcohols, fit on a single line (Fig. 6). The most serious exceptions to this general correlation are 2-methylpropan-2-ol and pentan-3-ol. These solvents are branched at the hydroxy group and, if hydrogen bonding is important, there might be important steric factors associated with organizing the solvent cage around the bis-oxonol. This becomes an even bigger problem for isomerization of the more sterically strained *cis* isomer.

Arrhenius plots were made for light-induced isomerization in several alkanols and were found to be linear in each case. Since viscosity can be described in terms of the following

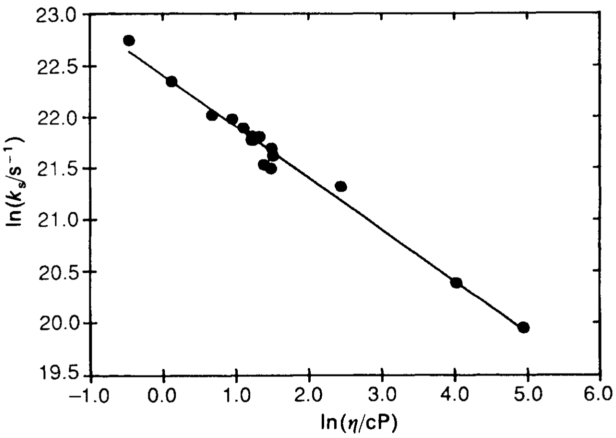

Fig. 6 Effect of solvent viscosity on the rates of light-induced isomerization for bis-oxonol **3** in a series of alkanol solvents at 22 °C

Table 3 Activation energies and inherent rates of twisting derived from Arrhenius plots made for bis-oxonol 3, in various solvents

	light-induced		thermal	
solvent	E_A /kJ mol^{-1}	$B/10^{12}$ s^{-1}	E_A /kJ mol^{-1}	$B/10^{11}$ s^{-1}
ethanol	15.4	2.7	38	5.7
butan-1-ol	15.6	2.9	38	6.1
hexan-1-ol	15.5	2.6	39	6.1
decan-1-ol	15.6	2.9	39	6.2
cyclohexanol	15.3	2.8	34	1.7
tert-butyl alcohol	16.2	3.2	42	12.5
isobutyl alcohol	15.3	2.7	35	1.7
acetonitrile	17.3	3.5	45	14.7

empirical equation[25]

$$\eta = \eta^0 \exp(E_\eta/RT) \tag{3}$$

where η^0 is the limiting viscosity at 0 K and E_η refers to the activation energy for viscous flow, the intercepts and slopes obtained from these Arrhenius plots can be used to derive estimates for B and E_A. The resultant values are collected in Table 3 and it is seen that both the activation energy and the inherent (activationless) rate of twisting of the rotor are only weakly dependent on the identity of the solvent. Again, alkanols that are sterically crowded at the hydroxy group might be considered as exceptions to the general behaviour. For 2-methylpropan-2-ol, for example, both the activation energy and the inherent rate of twisting are significantly higher than for linear alkanols and approach those found for aprotic solvents (Table 3). Such behaviour seems consistent with changes in the structure (or density) of the solvent cage and is indicative of the important role played by hydrogen bonding in controlling the mechanics of isomerization.

Photoisomerization in Aprotic Solvents

The photophysical properties of bis-oxonol 3 were measured in a series of polar organic solvents at 22 °C (Table 2). There are no obvious effects of solvent polarity, as measured in terms of the $E_T(30)$ parameter or the static relative permittivity, on either spectral parameters or rates of isomerization. There are, however, large variations in rates of photoisomerization among the different solvents that correlate reasonably well with changes in solvent viscosity (Fig. 7). From this correlation, both the power coefficient ($\alpha = 0.37 \pm 0.03$) and the intercept to Fig. 7 [*i.e.* $\ln(B - E_A/RT) = 21.70$] were found to be significantly smaller than those observed with protic solvents. It should also be recalled that the effects of rotor volume on the rates of photoisomerization are less pronounced in acetonitrile than in ethanol. These findings indicate to us that protic solvents promote photoisomerization and experience more pronounced microfriction, presumably due to hydrogen bonding to the bis-oxonol.

A linear Arrhenius plot was observed for light-induced isomerization in acetonitrile solution, allowing determination of E_A and B (Table 3). Relative to most alkanol solvents, both parameters are higher. Again, this finding appears to be indicative of hydrogen bonding lowering the barrier to photoisomerization but increasing frictional forces between rotor and adjacent solvent molecules. The latter may have the (apparent) effect of increasing the volume of the rotor while the former may be associated with slight differences in electron density (or bond order) at the isomerizing bond.

Thermal Isomerization in Alkanols

Similar studies were made for the thermal isomerization process, but it was observed that the rate of isomerization was not a simple function of solvent viscosity (Fig. 8). However, for the linear alkanols there was good correspondence between rate and viscosity. For such solvents, the power coefficient α was found to be 0.26 ± 0.02 whilst the intercept to Fig. 8 was 11.4 ± 0.08. In these solvents, it appears that the thermal process is less sensitive to changes in solvent viscosity (or microfriction) than is the corresponding photoisomerization. This finding appears consistent with the observed effects of the rotor volume on the rates of forward and reverse isomerizations. Rates of thermal isomerization measured in the branched alkanols and cyclohexanol (the *cis* isomer is not formed in glycerol) differ markedly from those found in linear alkanols, after allowing for changes in viscosity (Fig. 8). Solvents for which branching occurs at the hydroxy group (*i.e.* propan-2-ol, butan-2-ol, pentan-2-ol, pentan-3-ol and 2-methylpropan-2-ol) exhibit slower rates than expected by comparing their viscosity with that of the linear alkanols. This effect is attributed to steric blocking of the hydroxy group, an explanation which demands that hydrogen bonding promotes *cis* to *trans* isomerization. This hypothesis is supported by the observation that rates of thermal isomerization are much slower in aprotic than protic solvents of comparable viscosity (Table 2). The deviation

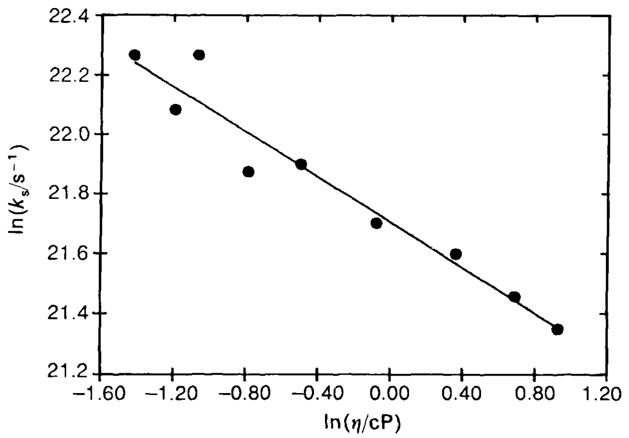

Fig. 7 Effect of solvent viscosity on the rates of light-induced isomerization for bis-oxonol 3, in a series of aprotic solvents (given in Table 2) at 22 °C

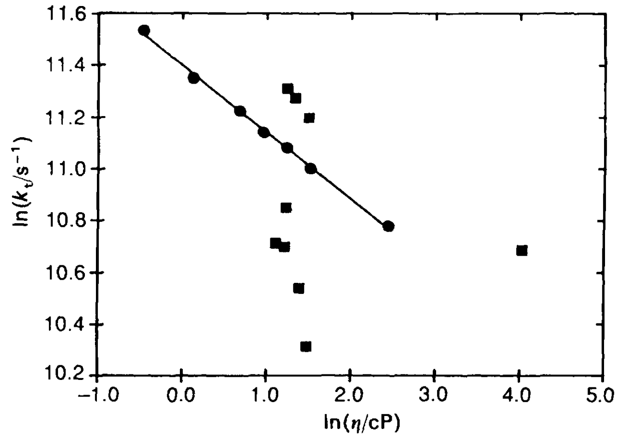

Fig. 8 Effect of solvent viscosity on the rates of thermal isomerization for bis-oxonol 3 in a series of linear (●) and branched (■) alkanol solvents at 22 °C

from expected rate (D) can be (crudely) expressed as

$$D = [k_t]_{obs}/(B/\eta^{\alpha})\exp(-E_A/RT) \qquad (4)$$

where $[k_t]_{obs}$ is the observed rate constant, $\alpha = 0.26$, and the parameter $[B\exp(-E_A/RT)]$ has a value of $9.1 \times 10^4\ s^{-1}$. As can be seen from Fig. 9, this factor correlates reasonably well with the steric coefficient for alkoxy substituents (v) as formulated by Charlton.[26] This correlation is consistent with hydrogen bonding between solvent and the *cis* isomer promoting isomerization to the stable *trans* form. Indeed, the rate of thermal isomerization observed for 2-methylpropan-2-ol ($k_t \approx 3 \times 10^4\ s^{-1}$), the most sterically blocked alkanol, still exceeds that expected in an aprotic solvent of equal viscosity ($k \approx 1 \times 10^4\ s^{-1}$; see below).

Interestingly, alkanols having a branch site remote from the hydroxy group (2-methylpropan-1-ol, 2-methylbutan-1-ol and 3-methylbutan-1-ol) exhibit a positive deviation from expected rate (*i.e.* $D > 1$). This cannot be explained in terms of steric hindrance at the hydrogen-bonding site but suggests that these alkanols present a lower density of solvent molecules around the rotor. This is a more subtle stereochemical effect and, possibly, provides for a larger cavity in which isomerization can occur. Cyclohexanol also gives a higher than expected rate of isomerization which might be associated with the manner in which the solvent packs around the rotor.

Linear Arrhenius plots were obtained for thermal isomerization in several alkanol solvents and the derived B and E_A values are compiled in Table 3. Inspection of these parameters shows that, relative to photoisomerization, the thermal isomerization step is characterized by a significantly higher activation energy and a slower inherent rate of twisting in a particular solvent. The differences noted between light-induced and thermal processes must relate to different electron densities (or bond order) at the isomerizing bond and to differing degrees of stereochemical strain in the reactants. For the thermal isomerizations, activation energies and inherent rates of twisting are essentially constant throughout the series of linear alkanols, but discrepancies occur for the other alkanols. For alkanols giving rise to anomolously fast rates of thermal isomerization (*i.e.* cyclohexanol and 2-methylpropan-1-ol) the activation energies are lower by *ca.* 5 kJ mol^{-1} while the inherent rates of twisting are only *ca.* 25% of those found in linear alkanols. In contrast, the sterically crowded 2-methylpropan-2-ol exhibits an activation energy and an inherent rate of twisting that appear somewhat higher than expected for the corresponding linear alkanol. These properties are attributed to changes in the extent of interaction between solute and solvent.

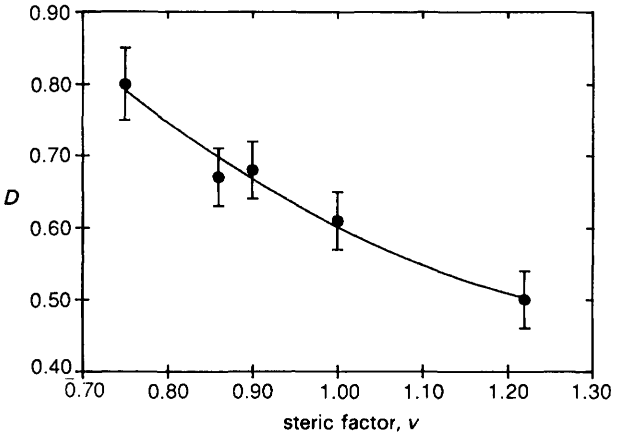

Fig. 9 Correlation between the deviation of observed rate of thermal isomerization for bis-oxonol **3** from the expected rate for a linear alkanol of the same viscosity and the steric factor for the solvent. The data were collected in (from left to right) propan-2-ol, butan-2-ol, pentan-2-ol, pentan-3-ol and 2-methylpropan-2-ol at 22 °C.

Thermal Isomerization in Polar Aprotic Solvents

The lifetime of the unstable *cis* isomer was measured in a series of aprotic solvents at 22 °C (Table 2). The rates of thermal *cis* to *trans* isomerization gave a reasonable correlation with solvent viscosity in these solvents, despite considerable scatter (Fig. 10). From the plot, the power coefficient $\alpha = 0.16 \pm 0.03$ and the intercept $[\ln(B - E_A/RT)]$ has a value of 10.00 ± 0.07. As noted above, the thermal isomerization process is less sensitive to microfriction with adjacent solvents than is the corresponding light-induced step and, again, there is a marked distinction between protic and aprotic solvents. The activation energy and inherent rate of twisting measured in acetonitrile (Table 3) are both significantly higher than the corresponding values found in protic solvents. In particular, the activation energy is *ca.* 6 kJ mol^{-1} higher and this difference must be a consequence of hydrogen bonding to the rotor in alkanol solvents. The increased inherent rate of twisting is indicative of the actual rotor having a smaller apparent volume and suggests less microfriction with adjacent solvent molecules.

Mechanics of Isomerization

According to transition-state theory, the non-adiabaticity factor for thermal isomerization must be *ca.* four-fold lower than that for the corresponding photoisomerization process to account for the derived B values. This seems surprising in view of the steric strain and non-planarity associated with the *cis* isomer since the thermal reaction might be expected to exhibit 'steric acceleration'. The results can be considered, however, in terms of the medium-enhanced barrier model[27] where it is assumed that the arrangement of solvent molecules around the solute is random with respect to the preferred geometric requirements for isomerization. As such, a certain proportion of solute molecules exist in solvent cages that provide unfavourable geometries for isomerization while the remaining solute is in solvent cavities that do not restrict rotation. Interconversion of the two conformations is considered to be rapid with respect to isomerization so that

$$B = k_{rot} K_m \qquad (5)$$

where k_{rot} is the rate of rotation within the solvent cavity and K_m is the equilibrium constant for interconversion between

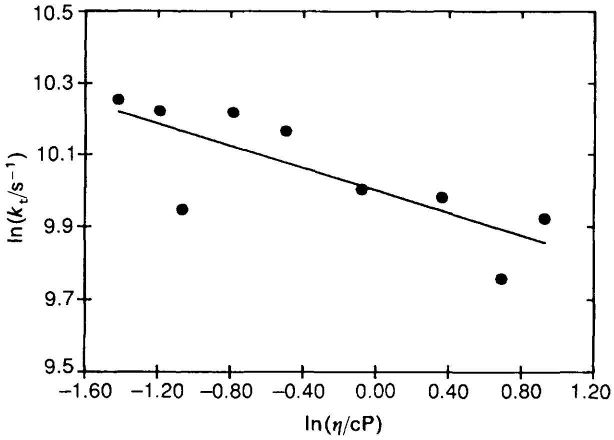

Fig. 10 Effect of solvent viscosity on the rates of thermal isomerization for bis-oxonol **3** in a series of aprotic solvents (given in Table 2) at 22 °C

the two types of solvent cage, provided K_m is small. Application of this model to the bis-oxonol case requires that K_m is smaller for the *cis* isomer than for the corresponding *trans* isomer. A further consequence of this model is that the power coefficient α can be equated to the fraction of the activation energy for viscous flow that is imposed by the solvent as an additional barrier to twisting of the rotor.[8]

Throughout this study, several key points prevail: (1) thermal isomerization is less sensitive towards microfriction with adjacent solvent molecules than is the corresponding light-induced step in any given class of solvents; (2) microfriction is less pronounced in aprotic than in protic solvents; (3) inherent rates of twisting are faster in aprotic than in protic solvents; (4) hydrogen bonding lowers the activation energies, despite probable increases in volume of the rotor; and (5) the viscosity and stereochemistry of the solvent influence the rates of isomerization at ambient temperature. Each of these findings relates to the extent of interaction between solvent and solute within the solvent cage. Hydrogen bonding to the bis-oxonol, which can occur at S, N or O atoms, increases the apparent volume of the rotor and provides for increased friction with the solvent reservoir. In order to explain the observed trend in activation energies and inherent rates of twisting, the extent of hydrogen bonding must increase in the order of proximally branched alkanols < linear alkanols < remotely branched alkanols. These effects are more pronounced for the sterically strained *cis* isomer where conjugation between the terminal oxonol subunits is less significant. We may surmise, therefore, that hydrogen bonding increases electron delocalization throughout the molecule and, thereby, reduces the bond order at the isomerizing bond.

This work was supported by the National Institutes of Health (CA 53619).

References

1 J. Davila, A. Harriman and K. S. Gulliya, *Photochem. Photobiol.*, 1991, **53**, 1.
2 D. L. Taylor, A. S. Waggoner, R. F. Murphy, F. Lanni and R. R. Birge, *Applications of Fluorescence in the Biomedical Sciences*, Alan R. Liss, New York, 1986.
3 *Methods in Cell Biology*, ed. D. L. Taylor and Y-L. Wang, Academic Press, New York, 1989, vol. 30.
4 I. A. Hemmila, *Applications of Fluorescence in Immunoassays*, Wiley-Interscience, New York, 1991.
5 Y-P. Sun and J. Saltiel, *J. Phys. Chem.*, 1989, **93**, 8310.
6 A. Harriman, *J. Photochem. Photobiol. A: Chem.*, 1992, **65**, 79.
7 J. E. I. Korppi-Tommola, A. Hakkarainen, T. Hukka and J. Subbi, *J. Phys. Chem.*, 1991, **95**, 8482.
8 Y-P. Sun, J. Saltiel, N. S. Park, E. A. Hoburg and D. H. Waldeck, *J. Phys. Chem.*, 1991, **95**, 10336.
9 K. Nakashima, T. Ando, T. Nakamizo and S. Akiyama, *Chem. Pharm. Bull.*, 1985, **33**, 5380.
10 F. C. Mohr and C. Fewtrell, *J. Immun.*, 1987, **138**, 1564.
11 T. J. Rink, C. Montecucco, T. R. Hesketh and R. Y. Tsien, *Biochim. Biophys. Acta*, 1980, **595**, 15.
12 A. C. Benniston, A. Harriman and K. S. Gulliya, *J. Chem. Soc., Faraday Trans.*, 1994, **90**, 953.
13 R. G. Shepherd, *J. Chem. Soc.*, 1964, 4410.
14 L. Pekkarinen and H. Linschitz, *J. Am. Chem. Soc.*, 1960, **82**, 2407.
15 J. K. Hurley, N. Sinai and H. Linschitz, *Photochem. Photobiol.*, 1983, **38**, 9.
16 A. J. Gordon and R. A. Ford, *The Chemist's Companion. A Handbook of Practical Data, Techniques, and References*, Wiley-Interscience, New York, 1972.
17 S. R. Meech and D. Phillips, *J. Photochem.*, 1983, **23**, 193.
18 S. J. Strickler and R. A. Berg, *J. Chem. Phys.*, 1962, **37**, 814.
19 N. S. Isaacs, *Physical Organic Chemistry*, Longman Group, Harlow, 1987.
20 A. Bondi, *J. Phys. Chem.*, 1964, **68**, 441.
21 S. P. Velsko, D. H. Waldeck and G. R. Fleming, *J. Chem. Phys.*, 1983, **78**, 249.
22 J. M. Hicks, M. T. Vanderall, E. V. Sitzmann and K. B. Eisenthal, *Chem. Phys. Lett.*, 1987, **135**, 413.
23 A. Spernol and K. Wirtz, *Z. Naturforsch., Teil A*, 1953, **8**, 522.
24 J. D. Simon and S-G. Su, *J. Phys. Chem.*, 1990, **94**, 3656.
25 Landolt-Bornstein, *Zahlenwerte und Functionen, Sechste Auflage, Band II, Teil 5*, Springer-Verlag, Berlin, 1969.
26 M. Charlton, *J. Org. Chem.*, 1978, **43**, 3995.
27 J. Saltiel and J. T. D'Aostino, *J. Am. Chem. Soc.*, 1972, **94**, 6445.

Paper 4/02348J; *Received* 20*th April*, 1994